Sensors & Transducers, Vol. 180, Issue 10, October 2014, pp. 198-205

Sensors & Transducers

Intelligent Test Mechanism Design of Worn Big Gear

[1] Hong-Yu LIU, [1] Ze-Ning XU, [2] Jun-Jie XI
[1] School of Mechanical Engineering and Automation,
University of Science and Technology Liaoning, Anshan, Liaoning Province, 114051, China
[2] School of Mechatronics Engineering, Zhengzhou Institute of Aeronautical Industry Management,
Zhengzhou, Henan Province, 450015, China
E-mail: lhy_12@126.com

Received: 9 July 2014 /Accepted: 30 September 2014 /Published: 31 October 2014

Abstract: With the continuous development of national economy, big gear was widely applied in metallurgy and mine domains. So, big gear plays an important role in above domains. In practical production, big gear abrasion and breach take place often. It affects normal production and causes unnecessary economic loss. A kind of intelligent test method was put forward on worn big gear mainly aimed at the big gear restriction conditions of high production cost, long production cycle and high-intensity artificial repair welding work. The measure equations transformations were made on involute straight gear. Original polar coordinate equations were transformed into rectangular coordinate equations. Big gear abrasion measure principle was introduced. Detection principle diagram was given. Detection route realization method was introduced. OADM12 laser sensor was selected. Detection on big gear abrasion area was realized by detection mechanism. Tested data of unworn gear and worn gear were led in designed calculation program written by Visual Basic language. Big gear abrasion quantity can be obtained. It provides a feasible method for intelligent test and intelligent repair welding on worn big gear. *Copyright © 2014 IFSA Publishing, S. L.*

Keywords: Big gear, Intelligent test mechanism, Polar coordinate equation, Rectangular coordinate equation, Laser sensor.

1. Introduction

When gear surface was worn, gear can not work normally. Gear work precision was affected. Vibrations and noises may be caused [1]. With the continuous development of science and technology, how to decrease gear abrasion and prolong gear service life is an important problem in industrial production [2]. Generally speaking, during gear transmission process, the material loss phenomenon of gear teeth contact surface belongs to abrasion research. For gear abrasion type, different country has different partition standard, for example German DIN3979 standard, American ANSI1010-E95 standard, International Standardization Organization ISO10825 standard and Chinese GB3481-83 standard. Generally speaking, main gear abrasion research contents contain gear abrasion influence factor, gear abrasion change law, wear resistance method and gear abrasion repair method. In these fields, lots of works were made by native and foreign scholars.

In gear abrasion test, under the invariable load and gear width ratio condition on some contact point, the pressures on every tooth profile contact point are nearly equal. Gear abrasion thicknesses are nearly equal. It was obtained by Huseyin Imrek [3]. The influences of rigidity and lubricant film thicknesses on gear surface abrasion were tested by mode detection method. Gear surface abrasion was estimated by vibration signal detection method. It was obtained by M. Amarnath [4]. Gear surface abrasion status was researched by testing lubricant oil temperature. The influence of lubricant oil temperature on gear surface abrasion status was estimated again. It was obtained by B. R. Hohn [5]. Gear surface point corrosion and gear vibration were researched. It can be known from vibration and ferrography technology that the more gear point corrosion, the more gear breach, the more gear vibration and the more gear abrasion. It was obtained by Wei Feng [6]. The relation between gear dynamic property and gear surface abrasion were researched. Finite element plasmodium method, simplified dispersed body method and worn gear surface model method were combined to accomplish above researches. The relation between gear surface abrasion and nonlinear dynamics of gear work was demonstrated based on multiple simulation results. It was obtained by Huali Ding [7]. Hypoid gear contact model was constructed. Abrasion simulation was made on hypoid gear by Archard abrasion model. Analyses were made by finite element method. Slither distance and contact pressure were calculated on every position of meshing surface according to simulation model. Slither distance calculation formula of gear surface meshing contact area was summarized. It was obtained by D. Paek [8]. The popularization and application of simulation technology decreases abrasion analysis complexity, saves research time, enhances work efficiency. It provides reference for deeper gear abrasion research.

In this paper, measure equations of straight involute gear under rectangular coordinates were derived. Gear abrasion test mechanism was designed. Gear abrasion quantity calculation program was written.

2. The Measure Equations Derivation of Straight Involute Gear under Rectangular Coordinates

Gear involute equations were expressed by polar coordinate equations in most data. Its derivation process is simple. It is accessible by reader. It is the base of other derivation and calculation. But it is inconvenient to gear abrasion test. The gear abrasion test in this paper needs to be made under rectangular coordinates. So, derivation and transformation of gear involute equations under polar coordinates were made. Gear involute equations under polar coordinates are shown as formula (1).

$$\begin{aligned} r_A &= \frac{r_B}{\cos\alpha_A}, \\ \theta_A &= tg\alpha_A - \alpha_A \end{aligned} \tag{1}$$

where r_A is the radius vector from A point to circle center. r_B is the gear base circle radius. α_A is the A point pressure angle. A point is an arbitrary point on gear involute under polar coordinates. Gear involute profile under rectangular coordinates is shown as Fig. 1. In Fig. 1, the connection straight line from base circle center to the intersection point of involute and base circle is x axis. The vertical upward straight line from base circle center is y axis. E point is an arbitrary point on gear involute. Curve EA represents a part of gear profile. Gear involute equations under polar coordinates can be transformed gear involute equations under rectangular coordinates. They are shown as formula (2).

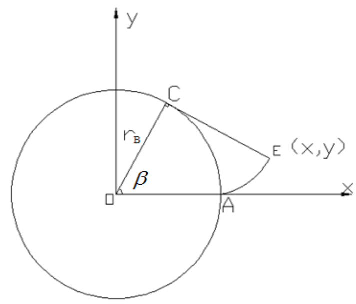

Fig. 1. Gear involute profile under rectangular coordinates.

$$\begin{aligned} x &= r_B\cos\beta + r_B\sin\beta \\ y &= r_B\sin\beta - r_B\cos\beta, \end{aligned} \tag{2}$$

where r_B is the base circle. β is the included angle of straight line OC and straight line OA in Fig. 1. Its unit is degree.

Rectangular coordinates with gear tooth groove centre line as its X axis was requisite in practical test. So, φ angle was revolved on above rectangular coordinates in a clockwise direction. X axis and Y axis correspond to new rectangular coordinates. It is shown as Fig. 2. After angle rotation, gear involute equations under new rectangular coordinates are shown as formula (3). After substituting formula (2) into formula (3), gear involute equations are shown as formula (4).

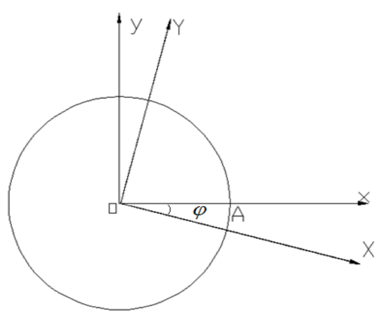

Fig. 2. New rectangular coordinates after revolving φ angle.

$$\begin{aligned} X &= x\sin\varphi + y\cos\varphi \\ Y &= x\cos\varphi - y\sin\varphi, \end{aligned} \tag{3}$$

$$\begin{aligned} X &= r_B(\cos\beta + \beta\sin\beta)\sin\varphi + r_B(\sin\beta - \beta\cos\beta)\cos\varphi \\ Y &= r_B(\cos\beta + \beta\sin\beta)\cos\varphi - r_B(\sin\beta - \beta\cos\beta)\sin\varphi \end{aligned}, \quad (4)$$

where r_B is the base circle. Its calculation formula is shown as formula (5).

$$r_B = \frac{mz\cos\alpha}{2}, \quad (5)$$

In formula (4), φ is the rotation angle of original rectangular coordinates. Its unit is radian. It equals to gear tooth groove angle half. Its calculation formula is shown as formula (6).

$$\varphi = \frac{s}{2r_B}, \quad (6)$$

where s is gear base circle tooth width. Its calculation formula is shown as formula (7).

$$s = m(\pi/2 - 2xtg\alpha - zinv\alpha)\cos\alpha, \quad (7)$$

where m is gear modulus. x is modification coefficient. α is gear reference circle pressure angle. Its unit is degree. After substituting formula (5) and formula (6) into formula (7), formula (8) can be obtained.

$$\varphi = \frac{\pi}{2z} - \frac{2x\,\mathrm{tg}\,\alpha}{z} - inv\alpha, \quad (8)$$

After substituting formula (8) into formula (4), formula (9) can be obtained.

$$\begin{aligned} X &= \frac{mz\cos\alpha}{2}\left[(\cos\beta + \beta\sin\beta)\sin\left(\frac{\pi}{2z} - \frac{2xtg\alpha}{z} - inv\alpha\right) + (\sin\beta - \beta\cos\beta)\cos\left(\frac{\pi}{2z} - \frac{2xtg\alpha}{z} - inv\alpha\right)\right] \\ Y &= \frac{mz\cos\alpha}{2}\left[(\cos\beta + \beta\sin\beta)\cos\left(\frac{\pi}{2z} - \frac{2xtg\alpha}{z} - inv\alpha\right) - (\sin\beta - \beta\cos\beta)\sin\left(\frac{\pi}{2z} - \frac{2xtg\alpha}{z} - inv\alpha\right)\right], \end{aligned} \quad (9)$$

Radian system is inconvenient than angle system. So, in order to convenient calculation, formula (9) was transformed into angle system. It is shown as formula (10).

$$\begin{aligned} X &= \frac{mz\cos\alpha}{2}\left[\left(\cos\beta + \frac{\pi\beta}{180^0}\sin\beta\right)\sin\frac{180^0}{\pi}\left(\frac{\pi}{2z} - \frac{2xtg\alpha}{z} - inv\alpha\right)\right. \\ &\quad \left. + \left(\sin\beta - \frac{\pi\beta}{180^0}\cos\beta\right)\cos\frac{180^0}{\pi}\left(\frac{\pi}{2z} - \frac{2xtg\alpha}{z} - inv\alpha\right)\right] \\ Y &= \frac{mz\cos\alpha}{2}\left[\left(\cos\beta + \frac{\pi\beta}{180^0}\sin\beta\right)\cos\frac{180^0}{\pi}\left(\frac{\pi}{2z} - \frac{2xtg\alpha}{z} - inv\alpha\right)\right. \\ &\quad \left. - \left(\sin\beta - \frac{\pi\beta}{180^0}\cos\beta\right)\sin\frac{180^0}{\pi}\left(\frac{\pi}{2z} - \frac{2xtg\alpha}{z} - inv\alpha\right)\right], \end{aligned} \quad (10)$$

Formula (11) and formula (12) can be obtained from Fig. 1.

$$\beta = \alpha_i + \theta, \quad (11)$$

$$\theta = tg\alpha_i - \alpha_i, \quad (12)$$

After substituting formula (11) into formula (12), formula (13) can be obtained.

$$\beta = tg\alpha_i, \quad (13)$$

After transforming radian into angle, formula (14) can be obtained.

$$\beta = \frac{180^0}{\pi}tg\alpha_i, \quad (14)$$

After substituting formula (14) into formula (10), formula (15) can be obtained.

$$\begin{aligned} X &= \frac{mz\cos\alpha}{2}\left[\left(\cos\frac{180^0}{\pi}tg\alpha_i + tg\alpha_i\sin\frac{180}{\pi}tg\alpha_i\right)\times\sin\frac{180^0}{\pi}\left(\frac{\pi}{2z} - \frac{2xtg\alpha}{z} - inv\alpha\right)\right. \\ &\quad \left. + \left(\sin\frac{180^0}{\pi}tg\alpha_i - tg\alpha_i\cos\frac{180^0}{\pi}tg\alpha_i\right)\times\cos\frac{180^0}{\pi}\left(\frac{\pi}{2z} - \frac{2xtg\alpha}{z} - inv\alpha\right)\right] \\ Y &= \frac{mz\cos\alpha}{2}\left[\left(\cos\frac{180^0}{\pi}tg\alpha_i + tg\alpha_i\sin\frac{180}{\pi}tg\alpha_i\right)\times\cos\frac{180^0}{\pi}\left(\frac{\pi}{2z} - \frac{2xtg\alpha}{z} - inv\alpha\right)\right. \\ &\quad \left. - \left(\sin\frac{180^0}{\pi}tg\alpha_i - tg\alpha_i\cos\frac{180^0}{\pi}tg\alpha_i\right)\times\sin\frac{180^0}{\pi}\left(\frac{\pi}{2z} - \frac{2xtg\alpha}{z} - inv\alpha\right)\right], \end{aligned} \quad (15)$$

Modulus and modification coefficient of standard involute straight gear can be known easily. Modification coefficient x is 0. It was substituted into formula (15), formula (16) can be obtained.

$$
\begin{aligned}
X = \frac{mz\cos\alpha}{2}\Bigg[&\left(\cos\frac{180^0}{\pi}tg\alpha_i + tg\alpha_i\sin\frac{180}{\pi}tg\alpha_i\right)\times\sin\frac{180^0}{\pi}\left(\frac{\pi}{2z}-inv\alpha\right) \\
&+\left(\sin\frac{180^0}{\pi}tg\alpha_i - tg\alpha_i\cos\frac{180^0}{\pi}tg\alpha_i\right)\times\cos\frac{180^0}{\pi}\left(\frac{\pi}{2z}-inv\alpha\right)\Bigg] \\
Y = \frac{mz\cos\alpha}{2}\Bigg[&\left(\cos\frac{180^0}{\pi}tg\alpha_i + tg\alpha_i\sin\frac{180}{\pi}tg\alpha_i\right)\times\cos\frac{180^0}{\pi}\left(\frac{\pi}{2z}-inv\alpha\right) \\
&-\left(\sin\frac{180^0}{\pi}tg\alpha_i - tg\alpha_i\cos\frac{180^0}{\pi}tg\alpha_i\right)\times\sin\frac{180^0}{\pi}\left(\frac{\pi}{2z}-inv\alpha\right)\Bigg],
\end{aligned}
\tag{16}
$$

3. Gear Abrasion Test Principle

The test principle diagram of gear abrasion surface drawn on gear cross section is shown as Fig. 3. In Fig. 3, straight line L_2 is the near tooth groove centre line of worn gear. The tooth groove was divided equally by straight line L_2. Two near gears are symmetrical about straight line L_2. Straight line L_1 is the centre line of worn gear. Worn gear was divided equally by straight line L_1. The distance straight line L_1 from and straight line L_2 is H. Laser sensor is on D point of straight line L_2. Laser sensor test route is a straight line perpendicular to straight line L_2. The straight line intersects straight line L_1 at C point. The straight line intersects unworn gear tooth involute at A point. The straight line intersects worn gear tooth involute at B point.

In worn gear surface test process, Laser sensor moves along straight line L_2 back and forth to realize gear abrasion test. The motion covers entire gear surface abrasion area. Laser sensor can test the distance from D point to B point. C point position can be obtained by calculated gear parameters. A point position can be obtained by substituting tested A point data into derived standard involute straight gear equations that is formula (16). Straight line DA distance is the difference between H and straight line AC. Gear surface abrasion quantity AB is the difference between straight line DB and straight line DA. Other point positions on gear cross section can be obtained in the same way. Gear worn surface test can be realized by this method.

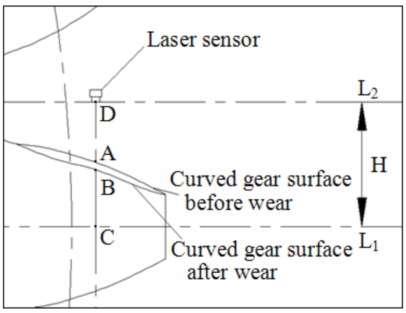

Fig. 3. The test principle diagram of gear abrasion surface.

In practical production, there is not law on gear surface abrasion. Gear surface abrasion is different with different working conditions. In order to dispose data conveniently, relative regular division was made on tested gear surface in this paper. The straight lines along gear width direction that is parallels with gear axis hole centre line and the curves along gear surface direction that is parallels with gear involute profile were used on division. n straight lines with same distance along gear width direction were selected. m straight lines with same distance along gear surface direction were selected. The distances between straight lines are equal to the distances between curves. Gear surface was divided n×m grids. It is shown as Fig. 4. In test, Laser sensor moves and tests along straight line and curves successively. Tested data are related to divided grids density. After test, n×m groups data can be obtained.

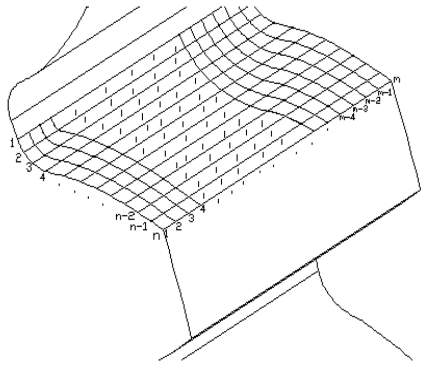

Fig. 4. Gear surface grids division diagram.

Tested data were given on rectangular coordinate form. X_{11} was named as X axis coordinate of grid test point on first row first column. Y_{11} was named as Y axis coordinate of grid test point on first row first column. Grid test point coordinate on first row first column was named as (X_{11}, Y_{11}). Other test point coordinates can be obtained by above method. Entire gear surface abrasion area can be tested and expressed with discrete points form. It provides theory base for intelligent gear surface test and intelligent gear surface repair welding.

4. Gear Test Localization

4.1. Gear Test Circle Center Localization

In order to realize test process, gear axis hole center need to be localized. It is very important to test coordinates localization, test mechanism localization and repair welding mechanism localization. At present there are two kinds of circle center localization methods. One is three points circle center localization. Another is least square method circle center localization. In three points circle center localization, arbitrary three points were selected on circle. Their coordinates are (x_1, y_1), (x_2, y_2) and (x_3, y_3) respectively. Circle center coordinate is (x_0, y_0). Circle radius is R. By this method, formula (17) can be obtained.

$$\begin{aligned}(x_1-x_0)^2+(y_1-y_0)^2&=R^2\\(x_2-x_0)^2+(y_2-y_0)^2&=R^2,\\(x_3-x_0)^2+(y_3-y_0)^2&=R^2\end{aligned} \quad (17)$$

After solving formula (17), relative circle center coordinate can be obtained. But obtained result by this method is inexact because of the big errors of gear coordinate point selections. In order to realize the approach between result and circle center position, least square method was adopted in this paper. Gear circle center coordinate was intercalated as (M, N). Then formula (18) can be obtained.

$$\left(x-M\right)^2+\left(y-N\right)^2=R^2, \quad (18)$$

After spreading and arranging formula (18), formula (19) can be obtained.

$$x^2-2Mx+M^2+y^2-2Ny+N^2=R^2, \quad (19)$$

It was intercalated that *m* is equal to *-2M*. *n* is equal to *-2N*. *p* is equal to the sum of M^2, N^2 and $-R^2$. Then formula (19) can be written as formula (20).

$$x^2+y^2+mx+ny+p=0, \quad (20)$$

In this paper, gear tooth number is z. So, z points were selected on selected circle. The coordinate of the *i* point is intercalated as $\left(x_i, y_i\right)$. d_i is the distance from the *i* point to circle center. Then formula (21) can be obtained.

$$d_i^{\,2}=\left(x_i-M\right)^2+\left(y_i-N\right)^2=x_i^2+y_i^2+mx_i+ny_i+p, \quad (21)$$

It was intercalated that δ_i is equal to $d_i^{\,2}$. Then formula (22) can be obtained.

$$\delta_i=x_i^2+y_i^2+mx_i+ny_i+p, \quad (22)$$

Then formula (23) can be obtained.

$$\sum\delta_i^2=\sum\left[\left(x_i^2+y_i^2+mx_i+ny_i+p\right)\right]^2, \quad (23)$$

When the value of $\sum\delta_i^2$ was taken as minimum value, x_i and y_i will illimitably approach the *i* point coordinate value on selected circle. After calculating parameters value of *m*, *n* and *p*, selected circle center coordinate that is gear circle center coordinate related the *i* point coordinate value can be obtained by formula (24).

$$\begin{aligned}X&=M=-\frac{m}{2},\\Y&=N=-\frac{n}{2}\end{aligned} \quad (24)$$

4.2. Gear Surface Test Mechanism Design

Gear surface test mechanism was designed in this paper. The three dimensional mode of gear surface test mechanism was constructed by Pro/E three dimensional design software. The assembly diagram of gear surface test mechanism and gear is shown as Fig. 5.

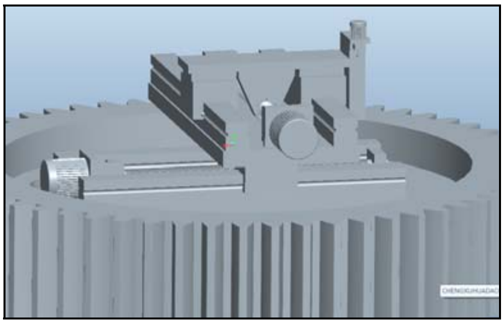

Fig. 5. The assembly diagram of gear surface test mechanism and gear.

The under part of gear surface test mechanism contains a ball screw, a lead rail, a motor and a work platform 1. Another set of ball screw, lead rail, motor and work platform was placed horizontally on work platform 1. Work platform 2 is perpendicular to work platform 1. Another set of ball screw, lead rail, motor and work platform was placed horizontally on work platform 2. Work platform 3 is vertical to work platform 2. The left and right motions of work platform 1 can be realized by adjusting work platform 1. The forward and backward motions of work platform 2 can be realized by adjusting work platform 2. The up and down motions of work platform 3 can be realized by adjusting work platform 3. The localization of entire test mechanism can be realized by this method. Sensor was adjusted to worn gear surface by adjusting the motors on work platform 1 and work platform 2. Sensor was localized on start test position according to divided grids. Then the motor on work platform 3 was opened. Test was made by sensor along gear width direction. Worn gear surface and unworn gear surface were all tested by the same method. The abrasion quantity of worn gear surface can be obtained by subtracting tested worn gear surface data from unworn gear surface data.

5. Sensor Selection

The tested information by sensor can be transformed to electrical signal form or other recognizable signal form. They were output to satisfy the requirements of transmission, processing, storage, record and show. Laser sensor was selected in this paper. Laser sensor is a kind of sensor testing by laser technology. Laser sensor can realize remote and contactless test. Its response speed is quick. Its precision is high. When laser sensor works, impulse was emitted by diode toward tested object. Impulse was reflected by tested object to laser sensor. Laser signal received by laser sensor was emitted to photoelectricity diode. The weak laser signal was amplified and transformed into relative electrical signal in photoelectricity diode. After processing relative electrical signal by computer, data test was accomplished. OADM 12 laser distance test sensor produced by Shanghai Peng Cheng Electronic Technology Limited Company was selected in this paper as gear surface test mechanism sensor. It is shown as Fig. 6.

Fig. 6. OADM 12 laser distance test sensor.

The basic parameters, electrical parameters, mechanical parameters, test precision and environment conditions of OADM 12 laser distance test sensor are shown as Table 1 ~ Table 5 respectively.

Table 1. Basic parameters.

Response element	**Tuning**	**Start pilot lamp**	**Camera lens polluted pilot lamp**	**Light source**	**Wave length (nm)**	**Laser grade**	**Light beam type**	**Light beam diameter (mm)**	**Interference suppression (ms)**
Direct row optical array	Button /outside	LED green	LED red /LED red quick flashing	Impulse red laser diode	675	2	Dot	0.2~0.5	<30

Table 2. Electrical parameters.

Response time /Release time (ms)	**Work voltage range (VDC)**	**Electricity attrition maximum (mA)**	**Output signal (mA)**	**Output circuit**	**Short circuit protection**	**Reversed polarity protection**
<0.9	12~28	100	4~20	Analog quantity	Yes	Yes

Table 3. Mechanical parameters.

Width/Diameter (mm)	**Height/Length (mm)**	**Depth (mm)**	**Type**	**Hull material**	**Front panel**	**Connector type**
12.4	37	34.5	rectangle	die casting zinc	glass	Union joint M8 4 needle

Table 4. Test precision.

Test distance (mm)	**Resolution (mm)**	**Linear error (mm)**	**Minimum self learning range (mm)**
16~26	0.002~0.005	±0.006~±0.015	> 1

Table 5. Environment conditions.

Operation temperature (°C)	**Protection grade**
0~50	IP67

6. Calculation Program Design

In order to enhance data processing efficiency and decrease personal error, Visual Basic programming language was adopted in this paper to design two calculation programs. By one calculation program, rectangle coordinate values of points on gear surface can be calculated according to variational pressure angle. Tested data of unworn gear and worn gear were led in another designed calculation program. Then big gear abrasion quantity can be obtained.

6.1. Rectangle Coordinate Calculation Program of Standard Involute Straight Gear

Formula (12) shows that rectangle coordinate values of points on gear tooth profile are relate to pressure angle of relative point, gear modulus, gear tooth number and gear pressure angle. The modulus, tooth number and pressure angle of tested gear are known variables. They can be inputted into program directly. The pressure angle of relative point is unknown variable. Four textboxes were designed on program main interface to input data in this paper. Input data are gear modulus, gear tooth number, gear pressure angle and tested point pressure angle separately. Another two textboxes were designed on program main interface to output calculation results. After inputting relative data, calculation button was pressed down. Relative X value and Y value under rectangle coordinates can be shown in two result output textboxes separately. After pressing down delete button, calculated data and improper input data can be deleted so as to input data again. After pressing down finish button, calculation program running was accomplished. The main interface of rectangle coordinate calculation program of standard involute straight gear is shown as Fig. 7.

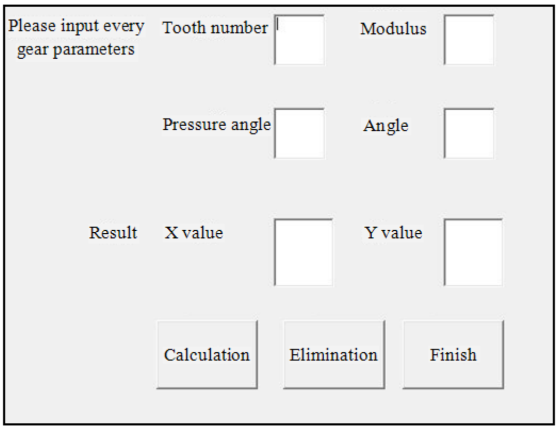

Fig. 7. The main interface of rectangle coordinate calculation program of standard involute straight gear.

6.2. Gear Abrasion Quantity Calculation Program

Two rows textboxes, two rows command keys and a row picture boxes were designed on gear abrasion quantity calculation program main interface. By pressing down five command keys on the third row, a set of tested worn gear data can be inputted into first row textboxes. By pressing down five command keys on the fourth row, a set of tested unworn gear data can be inputted into second row textboxes. The differences of inputted data between first row textboxes and second row textboxes can be shown in five picture boxes of the fifth row. The differences can be outputted with matrix form. By pressing down calculation key in the last row, above differences calculation results can be shown in five picture boxes of the fifth row. Big gear abrasion quantity calculation program main interface is shown as Fig. 8.

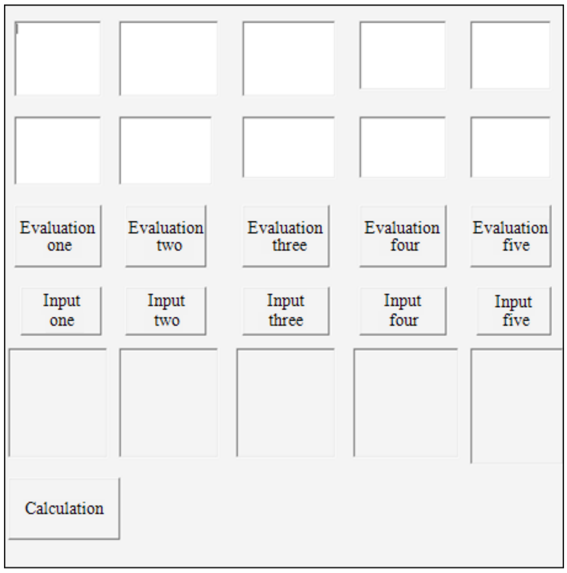

Fig. 8. Big gear abrasion quantity calculation program main interface.

7. Conclusions

A kind of intelligent test method was put forward on worn big gear. The measure equations transformations were made on involute straight gear. Original polar coordinates equations were transformed into rectangular coordinates equations. Transformed rectangular coordinates equations calculation program were written by Visual Basic language. According to big gear abrasion measure principle, big gear abrasion test mechanism was designed. After adjustment and positioning of big gear abrasion test mechanism, data collection on worn big gear surface can be realized by laser sensor. Tested data of unworn gear and worn gear were led in designed calculation program written by Visual Basic language. Big gear abrasion quantity can be obtained.

Acknowledgements

This work was supported by the Science and Technology Tackle Key Problem Plan Major Project of Henan Province (No. 102102210389) and the

Science and Technology Tackle Key Problem Plan Project of Henan Province (No. 082102230047).

References

[1]. Y. H. Mo, L. M. Zhang, S. B. Wang, Self-repairment of wearing in gear transmission, *Journal of Shanghai University Natural Science*, Vol. 17, Issue 1, 2011, pp. 90-93.

[2]. L. J. Zhao, H. Shi, Overview on gear transmission wear and its repair, *China Construction Machinery*, Vol. 5, Issue 2, 2007, pp. 243-247.

[3]. H. Imrek, H. Duzcukoglu, Relation between wear and tooth width modification in spur gears, *Wear*, Vol. 262, Issue 3-4, 2007, pp. 390-394.

[4]. M. Amarnath, C. Sujatha, S. Swarnamani, Experimental studies on the effects of reduction in gear tooth stiffness and lubricant film thickness in a spur feared system, *Tribology International*, Vol. 42, Issue 2, 2009, pp. 340-352.

[5]. B. R. Hohn, K. Michaelis, Influence of oil temperature on gear failures, *Tribology International*, Vol. 37, Issue 2, 2004, pp. 103-109.

[6]. W. Feng, X. P. Xie, Q. S. Liao, Experimental study of relation of wear and vibration in gear pitting failure, *Lubrication Engineering*, Vol. 32, Issue 11, 2007, pp. 69-73.

[7]. H. Ding, A. Kahraman, Interactions between nonlinear spur gear dynamics and surface wear, *Journal of Sound and Vibration*, Vol. 307, Issue 3-5, 2007, pp. 662-679.

[8]. D. Park, A. Kahraman, A surface wear mode for hypoid gear pairs, *Wear*, Vol. 267, Issue 9-10, 2009, pp. 1595-1604.